

Geophysical Research Letters



RESEARCH LETTER

10.1029/2019GL084281

Key Points:

- Global warming and urbanization exert important influences on both warm and cold days and nights in Eastern China
- Both anthropogenic and urban signals are detected in nighttime extreme temperatures while only the former is detected in daytime extremes
- The effect of urbanization is estimated to have contributed as much as one third of the observed warming in nighttime temperature extremes

Supporting Information:

- Supporting Information S1

Correspondence to:

Y. Sun,
sunying@cma.gov.cn

Citation:

Sun, Y., Hu, T., Zhang, X., Li, C., Lu, C., Ren, G., & Jiang, Z. (2019). Contribution of global warming and urbanization to changes in temperature extremes in Eastern China. *Geophysical Research Letters*, 46. <https://doi.org/10.1029/2019GL084281>

Received 27 JUN 2019

Accepted 21 SEP 2019

Accepted article online 22 OCT 2019

Contribution of Global warming and Urbanization to Changes in Temperature Extremes in Eastern China

Ying Sun^{1,2} , Ting Hu¹ , Xuebin Zhang³ , Chao Li⁴ , Chunhui Lu¹ , Guoyu Ren^{1,5} , and Zhihong Jiang² 

¹National Climate Center, Laboratory for Climate Studies, China Meteorological Administration, Beijing, China,

²Collaborative Innovation Center on Forecast and Evaluation of Meteorological Disasters, Nanjing University of Information Science & Technology, Nanjing, China, ³Climate Research Division, Environment and Climate Change

Canada, Toronto, Ontario, Canada, ⁴State Key Laboratory of Estuarine and Coastal Research, Key Laboratory of Geographic Information Science (Ministry of Education), School of Geographic Sciences, East China Normal University, Shanghai, China, ⁵Department of Atmospheric Science, School of Environmental Studies, China University of Geosciences, Wuhan, China

Abstract The anthropogenic-induced global warming and local urbanization exert important influences on temperature extremes in Eastern China. Here we use China station observations and climate models to investigate their effects on the warm and cold days and nights simultaneously. We quantified the contribution from these two factors based on an optimal fingerprinting method. We find that both anthropogenic and urbanization signals can be clearly detected and separated from each other in the nighttime temperature extremes. The effect of urbanization may explain as much as one third of the observed changes in cold and warm nights while the urbanization signal is weak in the daytime extremes. The results are robust against sampling uncertainty in the estimate of urbanization signal, but uncertainty due to collinearity between the urbanization signal and global warming is difficult to assess.

Plain Language Summary Understanding the causes behind changes in temperature extremes is of significance for reliably projecting future climate change. Previous studies have separately shown that global warming and the urbanization effects are the two important drivers for the increase of warm extremes and decrease of cold extremes in Eastern China. In this study, we consider these two factors simultaneously using an optimal fingerprinting method. We find that climate models can well reproduce the observed changes in extreme temperature when the urbanization effects are included. Both global warming and urbanization have contributed to changes in nighttime temperature extremes, with global warming contributing slightly more. On the other hand, changes in daytime temperature extremes seem to be predominantly due to global warming.

1. Introduction

Eastern China is the most populous and economically developed region in China and is significantly impacted by weather and climate extremes. For example, the summer of 2013 was the historically hottest at the time, and the heat and accompanying drought resulted in 59 billion RMB damage (Hou et al., 2014). Observations have shown that Eastern China has experienced an increase in extreme high-temperature events and a decrease in extreme low-temperature events since the mid-twentieth century (Lu et al., 2016; Wang et al., 2012; Yin et al., 2017; You et al., 2011). In particular, the past 10 years have witnessed frequent record-breaking high temperatures along with serious heat waves. It is projected that what was a rare heat wave in the historical record will become a usual event in the coming decades even under a median Representative Concentration Pathway (RCP)4.5 emission scenarios (Sun et al., 2014, 2018).

There are at least two major drivers contributing to the observed mean temperature-warming trend in China. One third of the observed mean temperature increase of 1.44 °C during the period 1961–2013, or about 0.49 °C, can be accounted for by the effect of urbanization that occurred since the middle 1980s (Sun et al., 2016). External forcing to the climate system, including large-scale anthropogenic influences, that is, human emissions of greenhouse gases and aerosols (referred to as anthropogenic forcing hereafter), and

©2019. The Authors.

This is an open access article under the terms of the Creative Commons Attribution License, which permits use, distribution and reproduction in any medium, provided the original work is properly cited.

natural external forcing including solar and volcanic activities can explain most of the remaining warming (Sun et al., 2016). As temperature extremes are ultimately related to mean temperatures, it follows that these two drivers must have also influenced extreme temperatures.

Previous studies have investigated the contributions to changes in extreme temperatures by individual drivers separately (Zhang et al., 2006). In a series of studies, Lu et al. (2016, 2018), Yin et al. (2017), Yin and Sun (2018) and Dong et al. (2018) found that the anthropogenic forcings exert clear detectable influence on intensity, frequency, and duration of temperature extremes represented by various temperature indices in China. The effect of urbanization, however, was not considered in these studies. As both anthropogenic forcing and urbanization cause regional warming in China, the regression approach that scales the regional temperature response to anthropogenic forcing to best match the observations, without explicitly considering the urbanization effect, could attribute at least some warming that is due to urbanization as a result of anthropogenic forcing.

Effects of urbanization on temperature extremes have been estimated by computing the difference in indices of temperature extremes between urban stations and rural stations (Zhang et al., 2011; Zhou & Ren, 2011). For this purpose, different methods have been used to estimate regional averages of extreme temperature indices for urban and rural areas by classifying observing sites into urban and rural stations (Ren et al., 2008, 2015; Ren & Zhou, 2014; Yang et al., 2011, 2017). Ren and Zhou (2014) used criteria including the population, station history, and the built-up size of the area to identify a fixed set of urban stations and rural stations. In their approach, a station is classified either as an urban station or as a rural station. The entire historical records for the urban stations are used to estimate averages of urban regions while those for rural stations are used to estimate rural averages. Because most of observing sites were established in inhabited regions, economic development of China has gradually urbanized what used to be rural areas. As a result, there is not a clear division between urban sites and rural sites. A rural site may have been urbanized to some degree; and thus, the differences between urban and rural sites may underestimate the urbanization effect. Yang et al. (2017) used the concept of dynamical classification of Yang et al. (2011) according to nighttime light data. In their approach, a station is considered as an urban station if the mean nighttime light values exceed a certain threshold and the urban land ratio is greater than 0.2 within a 7-km circular buffer area during 1978–2013. Regional averages for urban and rural areas are estimated based on variable set of stations each year. This approach makes an implicit underlying assumption that climate change and variability in the region is completely homogeneous in space and time such that the evolution of rural (or urban) areas does not result in any tangible differences in the rural and urban time series. As a result, this approach could potentially attribute some aspect of differences resulting from spatial and temporal variability of temperature extremes as an urbanization effect. Since the different approaches employed by Ren and Zhou (2014) and Yang et al. (2017) result in different sets of urban and rural stations, the regional mean series from these two sets of stations could differ. As a consequence, the effect of urbanization so identified would also differ. It should also be noted that sampling uncertainty in the estimates of urbanization effect, which can be quite large, was not evaluated in either approaches.

While it is straightforward to compute the difference series between rural and urban stations or between rural and urban and rural combined stations using the fixed-stations method of Ren and Zhou (2014) or variable-station method of Yang et al. (2011), there is not a simple interpretation for the difference series and, thus, the effect of urbanization estimated by these methods. This is because it is difficult to characterize the spatial representativeness of stations for urban and rural regions and to quantify the effect of sampling uncertainty in both space and time. Recognizing the difficulties in estimating the magnitude of urbanization effect on temperature and the fact that both urbanization and large-scale anthropogenic forcing contribute to temperature change, Sun et al. (2016) proposed a different method that estimates the effect of urbanization and large-scale anthropogenic forcing in tandem. This approach assumes that the pattern of the urbanization effect can be accurately estimated using the difference series and that models can simulate spatial and temporal patterns of anthropogenically forced temperature response correctly. The magnitudes of the effects of urbanization and anthropogenic forcings are estimated simultaneously from the observations and simulated responses to external forcings using an optimal fingerprint method. Here we use the Sun et al. (2016) method to attribute the observed changes in temperature extremes in Eastern China to urbanization and external forcings.

2. Data and Methods

2.1. Indices of Temperature Extremes

We consider four indices representing moderately extreme warm and cold temperature events. They are annual percentage of days when daily minimum temperature is greater than its ninetieth percentile (TN90p) or less than its tenth percentile (TN10p), as well as annual percentage of days when daily maximum temperature is greater than its ninetieth percentile (TX90p) or less than its tenth percentile (TX10p). These four indices have been used widely as they represent extreme events relative to daily temperature climatology (Zhang et al., 2011). Additionally, they have higher signal to noise ratio when compared with annual absolute extreme temperatures because many more daily observations are involved in their calculation.

2.2. Observational Data

We use the homogenized daily maximum and daily minimum temperatures at 2,419 stations in China to compute the temperature indices. These station data are provided by China National Meteorological Information Center (Xu et al., 2013). As historical simulations from the climate models end in 2012 (see below), and as station coverage was poor prior to the late 1950s, we use the time period 1958–2012 in this study. For more data information, please refer to supporting information.

We use the ETCCDI software (available from RCLimDex/FLimDex software package at <http://etccdi.pacific-climate.org/software.shtml>) to compute these indices to avoid data inhomogeneity caused by the use of a base period (Zhang et al., 2005). Regional averages of the observation series are obtained based on the station data. This involves three steps: 1) estimate station anomalies by removing the 1961–1990 mean from individual station series and 2) average station anomalies within $5^\circ \times 5^\circ$ grid boxes to obtain gridded anomalies. In total, there are 22 grid boxes used in the study. 3) Compute regional averages from the gridded values.

2.3. Indices From Climate Model Simulations

The same indices are also computed from daily outputs of simulations by the climate models participating in the Couple Model Intercomparison Project Phase 5 (CMIP5, Taylor et al., 2012). Indices computed by Sillmann, Kharin, Zhang, et al. (2013) and Sillmann, Kharin, Zwiers, et al. (2013) for historical and RCP experiments are used. These include one run for each climate model. Indices for other members of ALL forcing runs, for NAT forcing runs, or for control simulations were not used in Sillmann, Kharin, Zhang, et al. (2013) and Sillmann, Kharin, Zwiers, et al. (2013), they are computed separately using the code that generated the indices by Sillmann, Kharin, Zhang, et al. (2013). Historical ALL forcing simulations that end in 2005 were extended to 2012 using corresponding RCP4.5 runs. The model data used in the study are the same as those used in Lu et al. (2016). They include simulations driven by 1) historical anthropogenic and natural forcings (ALL) and the RCP4.5 forcing scenario, 2) the natural forcing only (NAT), and 3) the preindustrial experiments (CTL). The ALL experiments include 96 simulations from 21 models. The time period for these indices is 1958–2012. CTL simulations by 28 models are used to estimate internal climate variability. Model simulations are on different grids and are interpolated onto $5^\circ \times 5^\circ$ grid boxes that are consistent with the observations.

2.4. Estimate of Urbanization Signal Pattern

To determine the urban signal pattern (URB), we estimate regional averages for the urban and rural stations separately using the method described in section 2.2. Among all 1,641 stations in Eastern China (Supporting Information Figure S1), 86 stations are determined to be rural according to Ren and Zhou (2014). The remaining stations are regarded as urban stations in this paper. The URB signal is estimated by fitting a logistic sigmoid function to the difference between urban and rural series because the urbanization signal is expected to be a positive and monotonic increasing function. This signal pattern T_{URB} is finally used as the signal in the optimal fingerprinting approach described below.

2.5. Detection Method

To simultaneously detect the effects of anthropogenic forcing and urbanization on these temperature extreme indices in Eastern China, we use the optimal fingerprinting method based on a total least square method (Allen & Stott, 2003; Ribes et al., 2013; Sun et al., 2016). We regress the observational data onto the patterns of model simulated ALL response as well as the URB signal pattern such that

$$T_{\text{OBS}} = \beta_{\text{ALL}}(T_{\text{ALL}} - \nu_{\text{ALL}}) + \beta_{\text{URB}}(T_{\text{URB}} - \nu_{\text{URB}}) + \epsilon.$$

where T_{OBS} is a vector of observed temperature anomalies, T_{ALL} and T_{URB} are signal patterns for ALL and URB, ν_{ALL} and ν_{URB} are noise in the ALL and URB signal patterns, and β_{ALL} and β_{URB} are scaling factors (the regression coefficients). The ν_{ALL} is assumed to have the same form of model-simulated variability, with its variance inversely proportional to the number of model simulations used in the estimation of variability. It is not straightforward to estimate ν_{URB} . To ease the estimation of the scaling factors, we assume that there is effectively no uncertainty in the URB signal in the regression. This is done by assuming the variance to be equivalent to that of the average series from 1,000 model simulations. We, subsequently, separately consider the effect of sampling uncertainty in URB signal by conducting the detection and attribution analysis using each of the 1,000 bootstrap variations of the URB signal. As is generally considered in detection and attribution analyses (Allen & Stott, 2003; Ribes et al., 2013), a signal pattern is detected if its corresponding scaling factor is significantly greater than 0 at the 5% significance level. If in addition, this 90% confidence interval (CI) of the scaling factor also includes 1, it may be possible to attribute the observed changes to the signals if other plausible causes of the observed changes can be ruled out. The best estimates of the scaling factors adjust the ALL and URB signals to best match the observations, thereby enabling the estimation of the magnitude of ALL and URB signals in the observations simultaneously.

3. Results

3.1. Observed Changes in Warm and Cold Nights, the Urbanization Effects

The station map (Supporting Information Figure S1) in Eastern China shows a clear decrease of extreme cold days and nights (TX10p and TN10p) and an increase of extreme warm days and nights (TX90p and TN90p) in most stations, with smaller changes in daytime extremes (TX10p and TX90p) than in nighttime extremes (TN10p and TN90p). The upper portion of panels in Figure 1 shows the time series of eastern China averages for urban (black) and rural (yellow) stations, along with their difference (red) for the period 1958–2012. Changes in these series are consistent with median trends of individual station series. For the daytime extremes, the linear trends for the urban and rural stations are -0.54% per decade and -0.45% per decade for TX10p, 0.96% per decade and 0.95% per decade for TX90p, respectively. The linear trends in the difference series (red lines) of TX10p and TX90p are small, with a linear trend of -0.09% per decade for TX10p and 0.01% per decade for TX90p, respectively. For the nighttime extremes, the linear trends in the urban and rural series are -1.62% per decade and -1.1% per decade for TN10p and 2.06% per decade and 1.24% per decade for TN90p, respectively. The linear trends in the urban and rural difference series are quite large, at -0.52% per decade for TN10p and 0.82% per decade for TN90p, respectively. The urbanization effects can be clearly seen in the trends of the nighttime extremes. If the effect of urbanization is defined according to previous studies (e.g., Ren & Zhou, 2014) as the ratio between the difference in the trends of the urban and rural series and trends in the urban series, urbanization can explain the observed changes in nighttime extremes by 30% to 40%. These are larger than the estimates of urbanization effect on the same extremes for the whole country, which are between 18% and 28% according to Ren and Zhou (2014). The higher values in our estimates for Eastern China are reasonable, reflecting the fact that Eastern China has urbanized more strongly than the rest of the country because of more rapid and wider-spread development.

The lower portion of each panel in Figure 1 shows the sigmoid fit to the difference series. The sigmoid function fits the evolution of the urbanization effect well. The trends computed from the fitted curves and from the original series are of very similar values. Note that the urbanization signal in the daytime extremes is very small and flat, without any clear trends, in both the fitted curves and the original series. To estimate sampling uncertainty in the urban-rural difference series and corresponding sigmoid fits, we used a bootstrap procedure outlined in Sun et al. (2016). Here we divided Eastern China into $22\ 5^\circ \times 5^\circ$ grid boxes and computed difference series between urban and rural stations within each grid box for the four indices separately. We then sampled, with replacement, these grid box values to form 22 boxes to compute regional mean values. These regional means were then fitted to logistic curves. This procedure was repeated 1,000 times. The gray shading in the lower portion of Figure 1 shows the 5th to the 95th percentiles of the fit. It appears that the sampling error in the estimate of urbanization effect can be large.

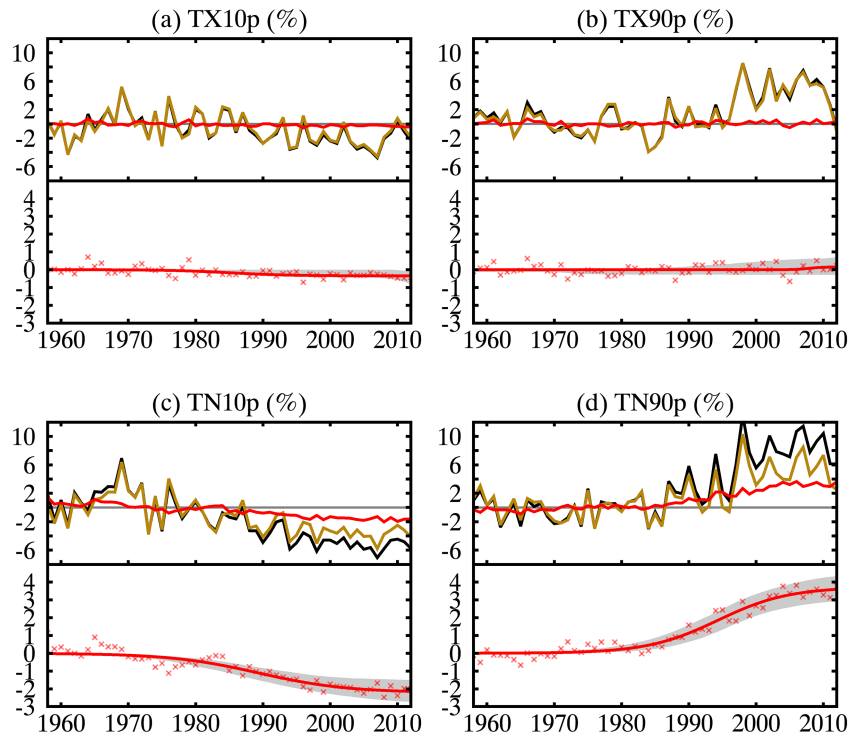


Figure 1. Upper portion of each panel: Time series of regional mean extreme temperature indices in Eastern China. Black and yellow lines are for urban and rural stations, respectively, while red line shows the difference between them. Lower portion of each panel: Difference between regional mean extreme temperature series of urban and rural stations. Red lines show sigmoid fits that are used as URB signal pattern in the detection and attribution analyses. The gray shading areas represent the 5th and 95th percentile ranges (gray areas) of the URB signal, estimated from the 1,000 bootstrap samples.

3.2. Comparison Between Observations and Simulations

Figure 2 displays the nonoverlapping 3-year mean series of the indices from the observations and simulations. The simulations under the ALL forcing generally reproduce the observed decrease in cold extremes and increase in warm extremes. For the daytime extremes, the simulations match the observations well with observations almost always at the center of the simulations. The URB signal is weak. For the nighttime extremes, the observed series are within the range of simulations but at the outer edge of simulations, indicating that while simulations are broadly consistent with observations, models tend to underestimate the observed decrease in cold nights and observed increase in warm nights. If the urbanization effect is removed from the observation, the match between the observations and simulations improves substantially.

3.3. Results From Detection and Attribution Analyses

Results from the two-signal detection and attribution analyses, by regressing observations onto the ALL and URB signals, are presented in Figure 3. For the daytime extremes, ALL is clearly detected with the fifth percent lower bound of the scaling factors above 0 while the URB signal is not detected. This means that external forcing has clearly affected these daytime extremes. The lack of detection of URB signal in daytime extremes can mean either a) effect of urbanization on daytime extremes is weak or b) the signal pattern constructed from the urban and rural differences is too weak to constrain the regression. As shown in Figure 2, simulations under ALL forcing track the observations well. It thus can be argued that the urbanization effect on daytime extremes may indeed be small, which would need to be verified by other studies that consider urbanization effect at a process level. For the nighttime extremes, both the ALL and URB signals are detected and they can also be separated from each other. This means that the effect of external forcing on these extremes can be identified with the consideration of the urbanization effect and vice versa. The best estimates of the scaling factors for ALL and URB signals are 0.83 (90% CI: 0.40–1.26) and 1.09 (90% CI: 0.26–1.92) for TN10p. They are 0.63 (90% CI: 0.16–1.12) and 1.23 (90% CI: 0.07–2.40) for TN90p, respectively. The fact

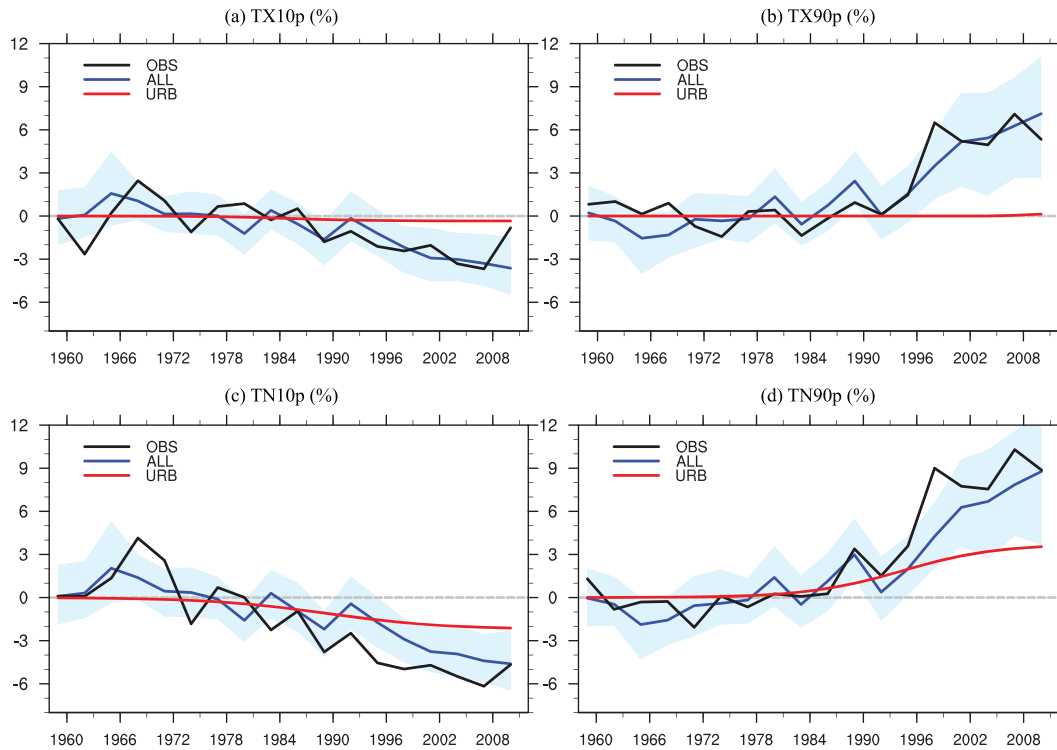


Figure 2. Regional mean 3-year nonoverlapping series for four extreme temperature indices from the observations (OBS), model simulated responses to all forcings (ALL), and the signal pattern for urbanization effect (URB). The URB is based on the sigmoid fits in Figure 1. Blue shading shows spread of the model-simulated responses to ALL forcings.

that the scaling factors for ALL are smaller than 1 from the two-signal analysis indicates that the models may still overestimate the observed changes in nighttime extremes even after the urbanization effect has been taken into account. Christidis et al. (2011) and Zwiers et al. (2011) found CMIP3 models tend to overestimate the most observed warming of nighttime extremes though this effect was less obvious in

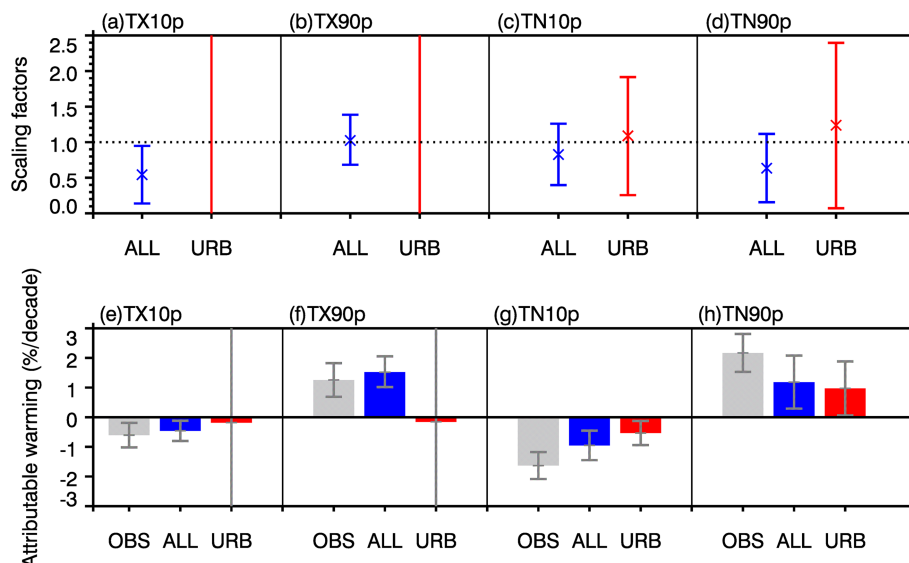


Figure 3. (a–d) Best estimates of scaling factors and their 5–95% confidence intervals for ALL and URB in two-signal analyses for the four temperature indices. (e–h) Observed trends for the extreme temperature indices and attributable changes, along with their 5–95% confidence intervals.

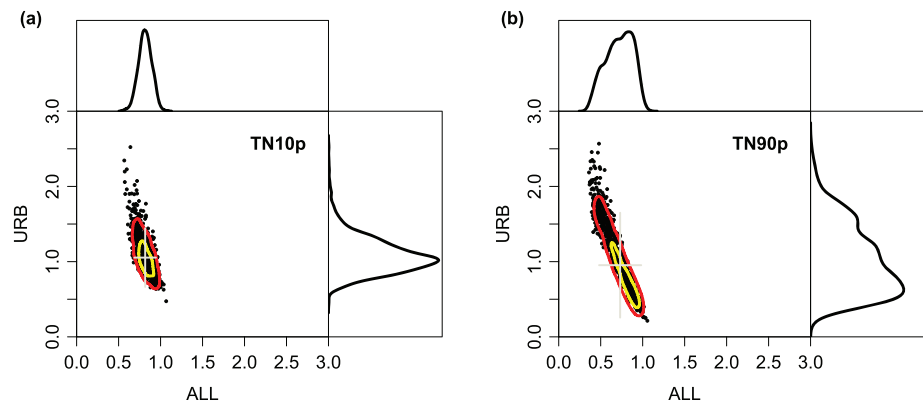


Figure 4. Scatter plots of ALL and URB scaling factors for TN10p (left) and TN90p (right) based on the 1,000 bootstrap samples of the URB signal. The joint 90% and 50% confidence regions are encircled by red and yellow curves, respectively. The gray lines represent 90% marginal confidence intervals. The marginal densities of the scaling factors are plotted on the top of (for ALL) or to the right of (for URB) the scatter plots.

CMIP5 models (Sillmann, Kharin, Zhang, et al., 2013). Morak et al. (2013) found similar results with HadGEM1 simulations. Both cloud and land processes in the models may have played a role but the exact cause of this is unclear.

We compute the attributable warming as the product between the linear trends in the noise-reduced model-simulated signals and the corresponding scaling factors. For the nighttime extremes, the observed trends, the estimated contributions from ALL, and URB for TN10p are -1.63% per decade (90% CI: -1.18% to -2.08%), -0.95% per decade (90% CI: -0.46% to -1.45%), and -0.53% per decade (90% CI: -0.13% to -0.94%), respectively. The corresponding values for TN90p are 2.17% per decade (90% CI: 1.53% to 2.81%), 1.18% per decade (90% CI: 0.29% to 2.08%), and 0.97% per decade (90% CI: 0.06% to 1.88%), respectively. This indicates that the urbanization effect explains about 33% and 45% of observed changes in TN10p and TN90p, respectively, assuming that other factors that might have affected trends are negligible. These are slightly higher than the estimates directly obtained from the difference series between urban (or urban and rural stations combined) and rural stations. Note however that these best estimates and confidence intervals are still subject to additional sampling uncertainty in the estimation of the URB signal, as we will see in the following subsection.

3.4. Robustness of Detection Results to Sampling Uncertainty

Figure 1 shows that the estimate of urbanization effect during the later decades may be subject to relatively large sampling uncertainty for the nighttime extremes. To examine the influence of this sampling uncertainty on detection and attribution analyses, we used each of the 1,000 bootstrapped estimates of the URB pattern in the two-signal detection and attribution analyses. For TN10p, the ALL and URB signals are detected 992 and 953 times. Both ALL and URB are simultaneously detected 948 times. For TN90p, the ALL and URB signals are detected 903 and 644 times with both signals simultaneously detected 547 times. Therefore, detection of the urbanization and global warming effects and their separation are both robust for nighttime temperature extremes, albeit more so for cold nights than warm nights.

Figure 4 displays scatter plots of the best estimate of ALL and URB scaling factors from the 1,000 bootstrap samples, along with their 90% and 50% confidence regions, as well as their marginal densities, for TN10p and TN90p (It should be pointed out that those are best estimates from each bootstrap sample, and they have their own confidence regions; the overall uncertainty shall be wider than illustrated by these confidence regions), respectively. Most of the best estimates of scaling factors fall in a well-defined region. The uncertainty range for ALL scaling factor is quite small, indicating relatively small influence due to sampling error in the URB signal estimate. The median values of the ALL and URB scaling factors for TN10p are 0.83 and 1.05, respectively, and those for TN90p are 0.73 and 0.95. As the median URB scaling is close to 1, it is reasonable to scale the estimated ALL signal down. Sampling uncertainty in the URB signal estimate likely contributed to the relatively small value of ALL scaling factor at 0.63

that was reported in section 3.3; nevertheless, ALL does still need to be scaled down to match the observations. Given these considerations, we conclude that urbanization effect on nighttime extreme temperature indices is substantial and may explain as much as one third of the observed warming in these indices. The strongest urbanization in China took place at the time of strongest warming in the global mean temperature, resulting in a strong collinearity between URB and ALL signals. This collinearity must have introduced additional uncertainty in our estimation. Nevertheless, given the considerations discussed above, uncertainty due to collinearity between the two signals should not qualitatively alter our above conclusion.

4. Conclusions

Previous studies have identified the anthropogenic forcing and urbanization as important factors contributing to the observed changes in moderate temperature extremes in Eastern China. These studies only consider one factor at a time, without taking the effect of the other factor into account. As the effects of urbanization and external forcing including the greenhouse gases and aerosols on temperature extremes are highly collinear, it can be difficult to know to what extent these estimates are affected by not considering the other factor. Here, we consider both effects in tandem by regressing the observations onto these two factors simultaneously. We find that the influence of anthropogenic forcing is clearly detected in the daytime extremes but changes in the size of the urbanization effect seem to be small. We also found that both external forcing and urbanization have played an important role in the observed changes in nighttime extremes. Simulations fit better with observations when the urbanization effect is considered, although the models tend to overestimate changes in these extremes even after accounting for urbanization. The urbanization effect on nighttime extremes is large, explaining perhaps as much as one third of the observed warming in these extremes. The results seem to be robust against sampling uncertainty in the estimate of urbanization effect. As the increase in nighttime extreme temperatures can exert serious impacts on human health, the added warming due to the continued urbanization in regions that are less urbanized today should be considered.

Acknowledgments

We thank Francis Zwiers and two anonymous reviewers for their very constructive comments. We acknowledge the Program for Climate Model Diagnosis and Intercomparison and the Working Group on Coupled Modeling of the World Climate Research Programme (WCRP) for their roles in making the WCRP CMIP multimodel data sets available. We thank the China National Meteorological Information Center for archiving the observational data (available at <http://data.cma.cn/>). This study was supported by the National Key R&D Program of China (2018YFC1507702), the National Science Foundation of China (41675074), and Climate Change Project (CCSF201905).

References

- Allen, M. R., & Stott, P. A. (2003). Estimating signal amplitudes in optimal fingerprinting. Part I: Theory. *Climate Dynamics*, *21*, 477–491. <https://doi.org/10.1007/s00382-003-0313-9>
- Christidis, N., Stott, P. A., & Brown, S. J. (2011). The role of human activity in the recent warming of extremely warm daytime temperatures. *Journal of Climate*, *24*, 1922–1930.
- Dong, S.-Y., Sun, Y., Aguilar, E., Zhang, X.-B., Peterson, T. C., Song, L.-C., & Zhang, Y.-X. (2018). Observed changes in temperature extremes over Asia and their attribution. *Climate Dynamics*, *51*, 339–353. <https://doi.org/10.1007/s00382-017-3927-z>
- Hou, W., Chen, Y., Li, Y., Wang, Y., Wang, Z., Zhu, X., & Zhao, L. (2014). Climatic characteristics over China in 2013. *Meteorological Monthly*, *40*, 491–501.
- Lu, C.-H., Sun, Y., Wan, H., Zhang, X.-B., & Yin, H. (2016). Anthropogenic influence on the frequency of extreme temperatures in China. *Geophysical Research Letters*, *43*, 6511–6518. <https://doi.org/10.1002/2016GL069296>
- Lu, C.-H., Sun, Y., & Zhang, X.-B. (2018). Multimodel detection and attribution of changes in warm and cold spell durations. *Environmental Research Letters*, *13*, 074013. <https://doi.org/10.1088/1748-9326/aacb3e>
- Morak, S., Hegerl, G. C., & Christidis, N. (2013). Detectable changes in the frequency of temperature extremes. *Journal of Climate*, *26*, 1561–1574.
- Ren, G.-Y., Li, J., Ren, Y.-Y., Chu, Z.-Y., Zhang, A.-Y., Zhou, Y.-Q., et al. (2015). An integrated procedure to determine a reference station network for evaluating and adjusting urban bias in surface air temperature data. *Journal of Applied Meteorology and Climatology*, *54*, 1248–1266. <https://doi.org/10.1175/JAMC-D-14-0295.1>
- Ren, G.-Y., & Zhou, Y.-Q. (2014). Urbanization effect on trends of extreme temperature indices of national stations over mainland China, 1961–2008. *Journal of Climate*, *27*, 2340–2360. <https://doi.org/10.1175/JCLI-D-13-00393.1>
- Ren, G.-Y., Zhou, Y.-Q., Chu, Z.-Y., Zhou, J.-X., Zhang, A.-Y., Guo, J., & Liu, X.-F. (2008). Urbanization effects on observed surface air temperature trends in North China. *Journal of Climate*, *21*, 1333–1348. <https://doi.org/10.1175/2007JCLI1348.1>
- Ribes, A., Planton, S., & Terry, L. (2013). Application of regularised optimal fingerprinting to attribution. Part I: Method, properties and idealised analysis. *Climate Dynamics*, *41*, 2817–2836. <https://doi.org/10.1007/s00382-013-1735-7>
- Sillmann, J., Kharin, V. V., Zhang, X.-B., Zwiers, F. W., & Bronaugh, D. (2013). Climate extremes indices in the CMIP5 multimodel ensemble: Part 1, model evaluation in the present climate. *Journal of Geophysical Research: Atmospheres*, *118*, 1716–1733. <https://doi.org/10.1002/jgrd.50203>
- Sillmann, J., Kharin, V. V., Zwiers, F. W., Zhang, X. B., & Bronaugh, D. (2013). Climate extremes indices in the CMIP5 multimodel ensemble: Part 2, future climate projection. *Journal of Geophysical Research: Atmospheres*, *118*, 2473–2493. <https://doi.org/10.1002/jgrd.50188>
- Sun, Y., Hu, T., & Zhang, X. B. (2018). Substantial increase in heat wave risks in China in a future warmer world. *Earth's Future*, *6*(11), 1528–1538. <https://doi.org/10.1029/2018EF000963>
- Sun, Y., Zhang, X., Zwiers, F. W., Song, L., Wan, H., Hu, T., & Ren, G. Y. (2014). Rapid increase in the risk of extreme summer heat in Eastern China. *Nature Climate Change*, *4*, 1082–1085. <https://doi.org/10.1038/nclimate2410>
- Sun, Y., Zhang, X.-B., Ren, G.-Y., Zwiers, F. W., & Hu, T. (2016). Contribution of urbanization to warming in China. *Nature Climate Change*, *6*, 706–709. <https://doi.org/10.1038/nclimate2956>

- Taylor, K. E., Stouffer, R. J., & Meehl, G. A. (2012). An overview of CMIP5 and the experiment design. *Bulletin of the American Meteorological Society*, 93, 485–498. <https://doi.org/10.1175/BAMS-D-11-00094.1>
- Wang, H.-J., Sun, J. Q., Chen, H. P., Zhu, Y. L., Zhang, Y., Jiang, D. B., et al. (2012). Extreme climate in China: Facts, simulation and projection. *Meteorologische Zeitschrift*, 21(3), 279–304. <https://doi.org/10.1127/0941-2948/2012/0330>
- Xu, W.-H., Li, Q.-X., Wang, X.-L., Su, Y., Cao, L.-J., & Feng, Y. (2013). Homogenization of Chinese daily surface air temperatures and analysis of trends in the extreme temperature indices. *Journal of Geophysical Research: Atmospheres*, 118, 9708–9720. <https://doi.org/10.1002/jgrd.50791>
- Yang, X.-C., Hou, Y.-L., & Chen, B.-D. (2011). Observed surface warming induced by urbanization in east China. *Journal of Geophysical Research*, 116, D14113. <https://doi.org/10.1029/2010JD015452>
- Yang, X. C., Ruby Leung, L., Zhao, N., Zhao, C., Qian, Y., Hu, K., et al. (2017). Contribution of urbanization to the increase of extreme heat events in an urban agglomeration in east China. *Geophysical Research Letters*, 44, 6940–6950. <https://doi.org/10.1002/2017GL074084>
- Yin, H., & Sun, Y. (2018). Detection of anthropogenic influence on fixed threshold indices of extreme temperature. *Journal of Climate*, 31(16), 6341–6352. <https://doi.org/10.1175/JCLI-D-17-0853.1>
- Yin, H., Sun, Y., Wan, H., Zhang, X.-B., & Lu, C.-H. (2017). Detection of anthropogenic influences on the intensity of extreme temperatures in China. *International Journal of Climatology*, 37, 1229–1237. <https://doi.org/10.1002/joc.4771>
- You, Q. L., Kang, S., Aguilar, E., Pepin, N., Flügel, W. A., Yan, Y., et al. (2011). Changes in daily climate extremes in China and their connection to the large scale atmospheric circulation during 1961–2003. *Climate Dynamics*, 36(11–12), 2399–2417. <https://doi.org/10.1007/s00382-009-0735-0>
- Zhang, X. B., Alexander, L., Hegerl, G. C., Jones, P., Tank, A. K., Peterson, T. C., et al. (2011). Indices for monitoring changes in extremes based on daily temperature and precipitation data. *Wiley Interdisciplinary Reviews: Climate Change*, 2(6), 851–870. <https://doi.org/10.1002/wcc.147>
- Zhang, X.-B., Hegerl, G. C., Zwiers, F. W., & Kenyon, J. (2005). Avoiding inhomogeneity in percentile-based indices of temperature extremes. *Journal of Climate*, 18, 1641–1651. <https://doi.org/10.1175/JCLI3366.1>
- Zhang, X.-B., Zwiers, F. W., & Stott, P. A. (2006). Multimodel multisignal climate change detection at regional scale. *Journal of Climate*, 19, 4294–4307. <https://doi.org/10.1175/jcli3851.1>
- Zhou, Y.-Q., & Ren, G.-Y. (2011). Change in extreme temperature events frequency over mainland China during 1961–2008. *Climate Research*, 50, 125–139. <https://doi.org/10.3354/cr01053>
- Zwiers, F. W., Zhang, X.-B., & Feng, Y. (2011). Anthropogenic influence on long return period daily temperature extremes at regional scales. *Journal of Climate*, 24(3), 881–892. <https://doi.org/10.1175/2010JCLI3908.1>